

Nd:YAG pumped nanosecond optical parametric oscillator based on LiInSe₂ with tunability extending from 4.7 to 8.7 μm

Georgi Marchev,¹ Aleksey Tyazhev,¹ Vitaliy Vedenyapin,² Dmitri Kolker,³ Alexander Yelisseyev,² Sergei Lobanov,² Ludmila Isaenko,² Jean-Jacques Zondy,⁴ Valentin Petrov¹

¹Max-Born-Institute for Nonlinear Optics and Ultrafast Spectroscopy, 2A Max-Born-Str. D-12489 Berlin, Germany, petrov@mbi-berlin.de

²Institute of Geology and Mineralogy, SB RAS, 43 Russkaya Str., 630058 Novosibirsk, Russia,

³Novosibirsk State Technical University, 20 K. Marx Pr., Novosibirsk, 630072, Russia and
Institute of Laser Physics (SB-RAS), 13/3 Lavren'teva Pr., Novosibirsk, 630090, Russia,

⁴Institut National de Métrologie, Conservatoire National des Arts et Métiers, 61 rue du Landy, F-93210 La Plaine St Denis, France

Abstract: LiInSe₂ is one of the few (only 5) non-oxide nonlinear optical crystals whose band-gap (2.86 eV) and transparency allowed in the past nanosecond optical parametric oscillation in the mid-IR without two-photon absorption for a pump wavelength of 1064 nm. However, the first such demonstration was limited to the 3.3-3.78 μm range for the idler and the average idler power did not exceed 2.5 mW. Here we report broadly tunable operation, from 4.7 to 8.7 μm, of an OPO based on LiInSe₂, achieving maximum idler pulse energy of 282 μJ at ~6.5 μm, at a repetition rate of 100 Hz (~28 mW of average power).

©2009 Optical Society of America

OCIS codes: (190.4970) Parametric oscillators and amplifiers; (190.4400) Nonlinear optics, materials

References and links

1. A. A. Kaminskii, "Laser crystals and ceramics: recent advances," *Laser Photon. Rev.* **1**, 93-177 (2007).
2. V. Petrov, F. Noack, I. Tunchev, P. Schunemann, and K. Zawilski, "The nonlinear coefficient d_{36} of CdSiP₂," *Proc. SPIE* **7197**, 7197-21/1-8 (2009).
3. E. O. Amman and J. M. Yarborough, "Optical parametric oscillation in proustite," *Appl. Phys. Lett.* **17**, 233-235 (1970).
4. D. C. Hanna, B. Luther-Davies, H. N. Rutt, and R. C. Smith, "Reliable operation of a proustite parametric oscillator," *Appl. Phys. Lett.* **20**, 34-36 (1972).
5. D. C. Hanna, B. Luther-Davies, and R. C. Smith, "Singly resonant proustite parametric oscillator tuned from 1.22 to 8.5 μm," *Appl. Phys. Lett.* **22**, 440-442 (1973).
6. Y. X. Fan, R. C. Eckardt, and R. L. Byer, "AgGaS₂ infrared parametric oscillator," *Appl. Phys.* **45**, 313-315 (1984).
7. P. B. Phua, R. F. Wu, T. C. Chong, and B. X. Xu, "Nanosecond AgGaS₂ optical parametric oscillator with more than 4 micron output," *Jpn. J. Appl. Phys.* **36**, L1661-L1664 (1997).
8. K. L. Vodopyanov, J. P. Maffettone, I. Zwieback, and W. Rudermann, "AgGaS₂ optical parametric oscillator continuously tunable from 3.9 to 11.3 μm," *Appl. Phys. Lett.* **75**, 1204-1206 (1999).
9. T.-J. Wang, Z.-H. Kang, H.-Z. Zhang, Q.-Y. He, Y. Qu, Z.-S. Feng, Y. Jiang, J.-Y. Gao, Y. M. Andreev, and G. V. Lanski, "Wide-tunable, high energy AgGaS₂ optical parametric oscillator," *Opt. Express* **14**, 13001-13006 (2006).
10. V. V. Badikov, A. K. Don, K. V. Mitin, A. M. Seregin, V. V. Sinaiskii, and N. I. Schebetova, "A HgGa₂S₄ optical parametric oscillator," *Quantum Electron.* **33**, 831-832 (2003) [transl. from *Kvantovaya Elektron.* **33**, 831-832 (2003)].
11. J.-J. Zondy, V. Vedenyapin, A. Yelisseyev, S. Lobanov, L. Isaenko, and V. Petrov, "LiInSe₂ nanosecond optical parametric oscillator," *Opt. Lett.* **30**, 2460-2462 (2005).
12. V. V. Badikov, A. K. Don, K. V. Mitin, A. M. Seryogin, V. V. Sinaiskiy, and N. I. Schebetova, "Optical parametric oscillator on an Hg_{1-x}Cd_xGa₂S₄ crystal," *Quantum Electron.* **35**, 853-856 (2005) [transl. from *Kvantovaya Elektron.* **35**, 853-856 (2005)].
13. J.-J. Zondy, V. Petrov, A. Yelisseyev, L. Isaenko, S. Lobanov, "Orthorhombic crystals of lithium thioindate and selenoindate for nonlinear optics in the mid-IR," In: *Mid-Infrared Coherent Sources and Applications*,

1. Introduction

Although room temperature lasing has been reported up to $\sim 5 \mu\text{m}$, practical solid-state-lasers have an upper limit of $\sim 3 \mu\text{m}$, with the most prominent representatives being the fixed wavelength Er^{3+} -lasers and the tunable Cr^{2+} -lasers [1]. The main difficulty with such lasers consists not only in finding suitable laser transitions with long living upper state but also in the exotic pump lasers required. However, the spectral range above $3 \mu\text{m}$ in the mid-IR can be continuously covered by nonlinear frequency down-conversion using powerful laser sources in the near-IR. Oxide crystals can be pumped by widely-spread high-power diode-pumped laser systems, such as Nd:YAG, and perform well up to $4 \mu\text{m}$, but their performance at longer wavelengths is dramatically affected by the onset of multi-phonon mid-IR absorption. Since nonlinear frequency conversion is intensity dependent process, high efficiency can be expected only using pulsed laser sources (femtosecond to nanosecond). At practical pump intensities, most of the chalcogenide mid-IR nonlinear crystals will suffer then two-photon absorption (TPA) at the pump wavelength of 1064 nm because of their low band-gap. In fact, there are only few candidates for such down-conversion devices pumped near 1064 nm , the properties of which were compared in [2] taking into account the TPA, residual absorption, birefringence, effective nonlinearity, thermal conductivity, and limitations related to the growth, availability and some opto-mechanical properties.

Although femtosecond and picosecond pulses are associated with much higher peak intensities, it is difficult to achieve simultaneously high output energies and conversion efficiency because of limitations related to the spectral acceptance or higher order dispersion and nonlinear effects. Thus nanosecond optical parametric oscillators (OPOs) seem to possess the best potential for achieving high average power and single pulse energy. Such OPOs, pumped in the $1 \mu\text{m}$ range, have been demonstrated, however, only with 5 of the 14 compounds analyzed in [2]: Ag_3AsS_3 [3-5], AgGaS_2 [6-9], HgGa_2S_4 [10], LiInSe_2 [11], and the solid solution $\text{Cd}_x\text{Hg}_{1-x}\text{Ga}_2\text{S}_4$ [12]. Moreover, apart from the archaic Ag_3AsS_3 [5], oscillation at idler wavelengths exceeding $4.4 \mu\text{m}$ has been demonstrated only with AgGaS_2 [8,9], achieving impressive tunability from 3.9 to $11.3 \mu\text{m}$ [8].

In this work we report broadband operation of a 1064 nm pumped LiInSe_2 (LISE) OPO, tunable from 4.7 to $8.7 \mu\text{m}$. Pumping at a repetition rate of 100 Hz and the absence of thermal effects allowed to increase the average power by more than an order of magnitude at wavelengths much longer than in the initial demonstration [11]. LISe is one of these few non-oxide nonlinear crystals whose band-gap (2.86 eV) and transparency allow operation in the mid-IR above $4 \mu\text{m}$ without TPA for a pump wavelength of 1064 nm . Unlike the AgGaS_2 (AGS) chalcopyrite which belongs to the same $A^I B^{III} C_2^{VI}$ ternary chalcogenide group, LISe crystallizes in the $\beta\text{-NaFeO}_2$ structure (orthorhombic $\text{mm}2$ symmetry). The interest in LISe is motivated by its superior thermo-mechanical properties [13]: isotropic expansion, thermal conductivity $\sim 5 \text{ W m}^{-1} \text{ K}^{-1}$ (~ 3 times higher than in AGS), and smaller thermo-optic coefficients as well as higher damage threshold than AGS, which are important for average power scaling.

2. Experimental set-up and LISe samples

The OPO cavity used is shown in Fig. 1. It consisted of two plane mirrors with a separation between 18.5 and 27.5 mm , depending on the LISe crystal used. The rear total reflector, TR, was an Ag-mirror (Balzers) with a reflection of $>98.5\%$ at the pump, signal and idler wavelengths. In the tuning ranges studies in the present work, the output coupler, OC, had a transmission of $18\text{-}22\%$ at the signal and $\sim 73\text{-}84\%$ at the idler wavelength, hence, the OPO can be considered as singly resonant with double pass pumping. However, the signal was not totally reflected by the output coupler to avoid extreme intracavity fluence that could damage

the crystals. The LiSe crystals were pumped through the output mirror which had a transmission of 82% at 1064 nm. The beams were separated by the pump bending mirror, BM, which had high reflection for the pump ($R=98\%$ for p-polarization) and transmitted $\sim 67\%$ (p-polarization) at the idler wavelengths, respectively. Both the plane-parallel output coupler, OC, and the bending mirror, BM, were on ZnSe substrates with uncoated rear surfaces.

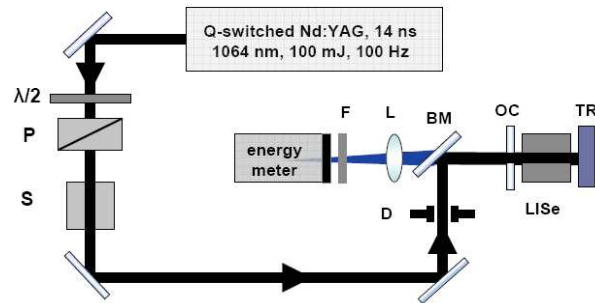


Fig. 1 Experimental set-up of the LiSe OPO. $\lambda/2$: half-wave plate, P: polarizer, S: mechanical shutter, F: $2.5 \mu\text{m}$ cut-on filter, L: 10 cm MgF_2 lens, D: diaphragm, BM: bending mirror, OC: output coupler, TR: total reflector.

The pump source was a diode-pumped and electro-optically Q-switched Nd:YAG laser (Innolas) optimized for a repetition rate of 100 Hz. According to the specifications, its linewidth amounts to 1 cm^{-1} , M^2 is <1.5 and the divergence is $<0.5 \text{ mrad}$. The laser generated 100 mJ, 14 ns (FWHM) pulses with an average power of 10 W. The measured energy stability was $\pm 1\%$. A mechanical shutter (S) with an aperture of 8 mm, operating up to 50 Hz (nmLaser), was employed to reduce the repetition rate and thus the average pump power. A combination of a half-wave plate, $\lambda/2$, and a polarizer, P, served to adjust the pump energy. The pump laser was protected by a Faraday isolator and the separation to the OPO was large enough to avoid feedback during the Q-switching process. The pump beam was not focused and had a Gaussian waist of $w \sim 1.9 \text{ mm}$ in the position of the OPO. The output of the OPO, behind the bending mirror, BM, was detected by a calibrated pyroelectric energy meter positioned in front of the focus of a 10-cm MgF_2 lens, L. Only the idler energy was measured, the residual pump radiation and the signal were blocked by a $2.5 \mu\text{m}$ cut-on filter, F.

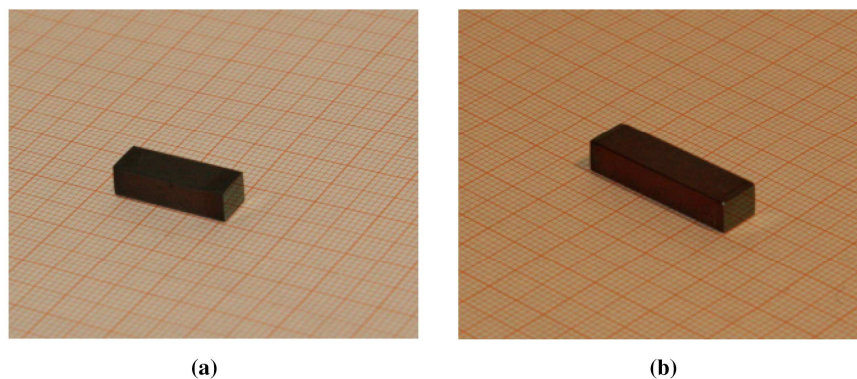


Fig. 2. AR coated samples of LiInSe_2 used in the present work: sample A (a) and sample B (b), see text.

The samples used in the present study, see Fig. 2, were grown from oriented seeds by the vertical two-zone furnace Bridgman technique. They were cut for propagation in the x - y plane,

type-II e-oe phase-matching, which is characterized by maximum effective nonlinearity d_{eff} [13]. One sample (A) was cut at $\varphi=41.6^\circ$ for idler wavelength $\sim 6.5 \mu\text{m}$ at normal incidence. It had an aperture of 5 mm (along z -axis) \times 6.5 mm and a length of 17.6 mm. This sample was AR-coated with a single layer for high transmission at 1064 nm and in the 1.15-1.35 μm signal range. We measured average surface reflectivity of 2.8% at 1064 nm and 1.8% at 1600 nm. From the measured transmission of 71% at 1064 nm and 85% at 1600 nm, we estimated effective absorption (including scatter) of 16%/cm at 1064 nm and 7%/cm at 1600 nm. The second sample (B) was cut at $\varphi=34^\circ$ for idler wavelength $\sim 8.8 \mu\text{m}$ at normal incidence. It had an aperture of 5 mm (along z -axis) \times 7 mm and a length of 24.5 mm. This sample was AR-coated with the same single layer for high transmission at 1064 nm and in the 1.15-1.35 μm signal range. However, due to some failure in the coating process, the difference in the residual reflectivity of the two surfaces was more pronounced. One surface had substantially higher (5% at 1064 nm and 4.5% at 1600 nm) reflection than the other (1% at 1064 nm and $<1\%$ at 1600 nm). These values should be compared to the Fresnel reflection of 15.8% per surface due to the refractive index of 2.32 at a signal wavelength of 1.25 μm . From the measured transmission of 67.7% at 1064 nm and 82% at 1600 nm, we estimated for sample B, effective absorption (including scatter) of 14%/cm at 1064 nm and 6%/cm at 1600 nm, which are very similar to the estimates for sample A.

3. Results and discussion

We studied the input/output characteristics of the OPO, including the oscillation threshold, at normal incidence and minimum possible cavity length. The tuning curves required tilting of the crystals and the corresponding cavity length was slightly increased.

The thresholds measured for cavity length of 18.5 mm (sample A) and 25.5 mm (sample B) amounted to 6.8 mJ and 7.9 mJ, energy incident on the crystals, respectively. These values correspond to average fluence of 0.06 J/cm² and 0.07 J/cm² or pump intensity of 4.3 MW/cm² and 5 MW/cm². The peak on-axis values for the fluence and the intensity are two times higher. The threshold can be calculated by using Brosnan & Byer's formula [14] for a singly resonant OPO with recycled pump. We used the exact experimental parameters, correcting for the pump beam absorption after the first pass and assuming equal (averaged for signal and idler) absorption of 0.05 cm⁻¹ for the resonated wave. From the nonlinear coefficients of LiSe, rescaled using Miller's rule [2], we calculated an effective nonlinearity of $d_{\text{eff}}=10.6 \text{ pm/V}$ ($\varphi=41.6^\circ$, sample A) and 11 pm/V ($\varphi=34^\circ$, sample B). The results for the threshold pump fluence were 0.23 J/cm² and 0.15 J/cm² for sample A and B, respectively. These values correlate better with the experimental peak (on-axial) values which can be explained by the fact that oscillation starts in the central part of the pump beam. Deviations and the fact that sample B had in fact a higher oscillation threshold than sample A may have several reasons: the losses at the exact signal and idler wavelengths were unknown and we interpolated them to 6%cm⁻¹ at the signal and assumed 4%cm⁻¹ at the idler wavelength in accordance with [11], eventually these losses, in particular for sample B, could be higher; besides for the pump, the residual reflections at the crystal faces were neglected; and finally the partial resonance of the idler is not taken into account by the theory. Having in mind all such assumptions, the correspondence between theory and experiment can be considered as satisfactory.

At a pump level of about two times the pump threshold we investigated the dependence of the output power on the repetition rate in the range 10-100 Hz. Fluctuations were within the experimental error and we conclude that there is no such dependence. This result was rather unexpected since the present samples had in fact larger residual absorption than the one used in the initial work [11] at shorter idler wavelengths. This fact can be explained by the weaker thermal lensing in the case of larger beam sizes. The measurements were performed at 100 Hz with the shutter removed (Fig. 1).

The input/output characteristics for the two samples are shown in Fig. 3a. Maximum energies of 282 μJ at 6.514 μm and 116 μJ at 8.428 μm were measured. These values correspond to external quantum conversion efficiencies of 10.3% and 4.3%, respectively. The above wavelengths deviate from the calculated ones being longer for sample A and shorter for

sample B. However, the deviations at the signal wavelengths, from the measurement of which the idler wavelengths were calculated, were only about 3 nm and 5 nm, respectively. The maximum average power at 100 Hz amounts to 28 mW. This is an improvement of more than an order of magnitude in comparison to our initial work, where ~2.5 mW at 3457 nm were achieved at lower repetition rates [11]. Since OPO operation with any chalcogenide crystal is confined to a narrow pump power range between the oscillation threshold and the damage threshold this fact emphasizes the importance of the good spatial profile and the pulse-to-pulse stability of the diode-pumped pump source.

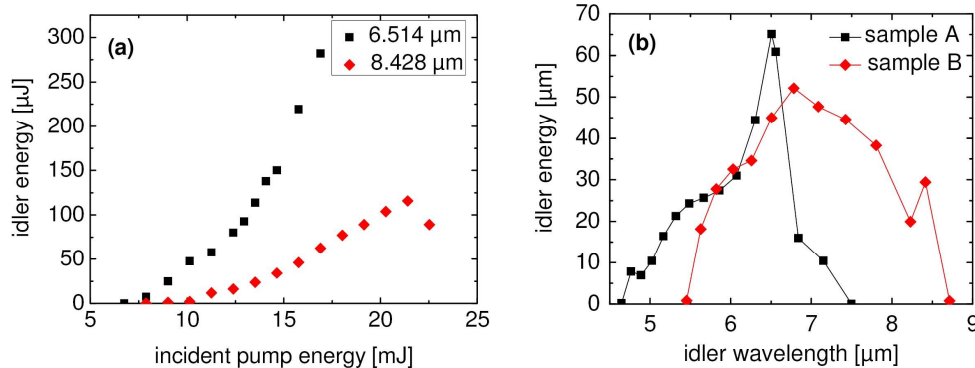


Fig. 3. (a) Output idler energy with LISe sample A (black squares) and sample B (red diamonds) versus pump energy at 1064 nm, incident on the crystals. The curves are recorded at normal incidence with cavity lengths of 18.5 and 25.5 mm, respectively. The last point in case B denotes a surface damage. (b) Tuning OPO curves recorded for the two LISe samples at fixed pump energy.

The OPO linewidth was measured at the signal wavelength of 1272 nm using a 1-mm-thick Ag-coated CaF_2 Fabry-Perot etalon. It was ~ 58 GHz ($\sim 1.9 \text{ cm}^{-1}$). This is 2 times less than the spectral acceptance for the three-wave nonlinear process assuming narrow-band pump. The pulse-to-pulse stability for the idler pulses measured at maximum output level was $\pm 5\%$. The pulse duration at the same signal wavelength measured with a fast (0.7 ns) InGaAs photodiode was 7 ns.

The tuning curves (Fig. 3b) were recorded by lengthening the cavity to 20.5 mm (sample A) and 27.5 mm (sample B) and tilting the crystals in the critical plane (rotation about the z-axis). The pump energy was 11.8 mJ for sample A and 16.9 mJ for sample B. Note that the upper limit of the tunability is determined by the LISe absorption which, for such sample lengths, sets on from about 8 μm , and is not related to the optics used (the thin MgF_2 lens was substituted by a BaF_2 lens to check this). The point which deviates from the smooth dependence for sample B is near 8.428 μm , corresponding to normal incidence, which can be explained by some enhancement of the feedback by the partial reflection of the crystal faces. Thus we showed that the full transparency range of LISe can be utilized using an OPO pumped at 1064 nm, however, in order to extend the tunability up to 12 μm and more, shorter crystal samples will be needed in addition to reduction of the residual crystal loss. This in turn means that the OPO should be operated at higher pump levels which will require solution of the surface damage problem.

Surface damage was observed with both OPO active elements and studied also with four 1 mm thick plates of LISe, cut in the same direction as sample B. Two of these plates were only polished and the other two had the same kind of AR coating on one of their faces only. The results of the extracavity damage tests at 1064 nm using the same pump source without focusing can be summarized as follows.

For uncoated and AR-coated LISe plates, complete damage (surface and crack) occurs for 14 ns long pulses at 1064 nm and 100 Hz within seconds/minutes for 44-52 mJ incident energy, on-axial fluence of 0.78-0.92 J/cm^2 (56-66 MW/cm^2 peak on-axis pump intensity).

In several cases irreversible whitened spots (surface deterioration) were observed starting from 29 mJ pump at 100 Hz, corresponding to an on-axis fluence of 0.5 J/cm^2 or 36 MW/cm^2 of peak on-axis intensity. This is the minimum fluence value for which such kind of damage was observed, and there is obvious dependence on the position and the sample. For increasing pump levels, the whiter spots changed slightly in diameter and preserved their colour, until complete damage occurred. The whiter spots occur on uncoated surfaces, however, they occur also on AR-coated surfaces, presumably beneath the layer. In most of the cases they occurred at higher pump energies and in one of the uncoated test plates they did not occur at all, until complete damage was observed at 52 mJ which seems to indicate that this effect is related to the polishing/coating procedure because all samples were from the same LISe boule.

No reliable information could be obtained on gray track formation which seems not to be the limiting factor in the temporal regime studied. However, many point defects could be seen with a microscope in all samples, inside the bulk and on the surface. Their concentration differs and maybe correlates with the different damage thresholds observed.

In principle the AR-coating applied seems to be sufficiently resistant for OPO operation and in some cases the surface damage threshold was higher for the AR-coated surface. But the quality of the coating is not reproducible as evidenced in the OPO experiment, in which always one of the surfaces (the one with higher residual reflection) got damaged at lower pump levels, independent whether it was a front or rear surface with respect to the pump. It can be only speculated why damage of the two OPO samples in the form of whiter surface spot occurred at much lower pump energy (10-15 mJ) when inside the cavity. Complete damage was also observed at lower levels (15-20 mJ) but could be a consequence of already existing whiter spot. There are two possibilities: either contribution from the resonated signal wave (as reported for other crystals [8]) or simply low quality of this AR-coating. Experiments outside the cavity indicated lower damage of the surface with higher residual reflection, also lower threshold for whitening, so it seems more probable that this surface was simply of lower quality and that is why it got damaged although it was not always the front surface in the OPO. Comparing the results with coated and uncoated surfaces one can expect that, for the present quality of the grown material, optimization of the AR-coating process could allow the safe use of peak on-axis intensities of about 50 MW/cm^2 or incident pump energy of roughly 40 mJ.

4. Conclusions

In summary, we demonstrated for the first time to our knowledge nanosecond OPO operation with LISe crystal in the mid-IR wavelength range above $4 \mu\text{m}$ extending up to $8.7 \mu\text{m}$ for the idler wave. The maximum idler pulse energy of $282 \mu\text{J}$ at $\sim 6.5 \mu\text{m}$ corresponds to an average power of $\sim 28 \text{ mW}$ at a repetition rate of 100 Hz. This compares well with the $372 \mu\text{J}$ at $6 \mu\text{m}$ reported with an AGS OPO [8]. Further scaling is possible provided better polishing and AR-coating processes are developed. One of main challenges remains, however, the reduction of the residual losses in the clear transparency range of LISe because only after solving this problem the better thermo-mechanical characteristics of this material will allow to outperform the more conventional chalcopyrite AGS.

Acknowledgments

The research leading to these results has received funding from the European Community's Seventh Framework Programme FP7/2007-2011 under grant agreement n° 224042. We acknowledge also support from DLR (International Bureau of BMBF) under project RUS 08/013 and from DAAD, Michail-Lomonosov-Programme (D. K.).